Periodically-segmented liquid crystal core waveguides

2017 J. Phys. D: Appl. Phys. 50 385107

(http://iopscience.iop.org/0022-3727/50/38/385107)

IOP Publishing Journal of Physics D: Applied Physics
J. Phys. D: Appl. Phys. **50** (2017) 385107 (5pp) https://doi.org/10.1088/1361-6463/aa83f1

Periodically-segmented liquid crystal core waveguides

Mukesh Sharma[1], **M R Shenoy and Aloka Sinha**

Department of Physics, Indian Institute of Technology Delhi, Hauz Khas, New Delhi-110 016, India

E-mail: mukeshnice@gmail.com

Received 16 May 2017, revised 12 July 2017
Accepted for publication 3 August 2017
Published 31 August 2017

Abstract

We report the fabrication and characterization of electrically-tunable periodically segmented waveguides (PSWs) with different duty cycles of 0.25, 0.33, 0.50 and 0.76, using the nematic liquid crystal 5CB as the guiding layer, and the negative photoresist AZ15nXT as the cladding. The experimental results show that light diffracts and re-focuses periodically on propagation through the liquid crystal (LC) core PSW, when an external voltage is applied to the periodically segmented electrodes. The performance of the fabricated LC core PSWs are analyzed in terms of effective refractive index, output power and duty cycle. The electrically-tunable LC core PSWs have potential application in the realization of optical filters, polarizers and dynamic mode size converters.

Keywords: liquid crystal devices, periodically-segmented waveguide, electrooptic devices

(Some figures may appear in colour only in the online journal)

1. Introduction

Periodically segmented waveguides (PSWs) have attracted considerable attention for linear and nonlinear optical applications in integrated optics [1–9]. In its simplest form, a PSW consists of a linear array of high-index regions, surrounded by lower-index regions, forming an optical waveguide (see figure 1). δ is the length of the high-index segment, and Λ is the period of segmentation; the duty cycle (γ) is given by $\gamma = \delta/\Lambda$. There have been several reported experimental and numerical studies of segmented waveguides in $KTiOPO_4$ [2, 3] and $LiNbO_3$ [5–12]. Some of the reported methods to realize PSWs include ion-exchange and femtosecond laser inscription [2–9]. The linear propagation characteristics of PSWs have been analyzed by Bierlein *et al* [2], Li and Burke [4], Thyagarajan *et al* [5], and Weissman and Hardy [9]; it was shown that the PSWs can be represented by an equivalent uniform waveguide to determine the propagation characteristics. The high birefringence and inherent electro-optic properties of liquid crystal (LC) materials have been exploited to fabricate optical gratings, waveguide based optical switches [13–21] and photonics devices [22–25]. Recently, we reported fabrication of the first LC core PSW using the liquid crystal 5CB as the guiding medium [26]. The LC core PSWs were fabricated by applying an external electric field to the pre-imprinted periodically segmented electrode pattern on an ITO-coated glass substrate. The PSWs fabricated using LC material have certain advantages compared to the PSWs in other anisotropic materials; the electrically-tunable refractive index of the LC core segments provide dynamic control over the propagation characteristics. These LC core PSWs can be further used to realize waveguide based devices such as wavelength filters, mode size converters, Bragg reflectors and polarizers with tunable characteristics.

In this paper, we present experimental and numerical results on the propagation characteristics of LC core PSWs, fabricated on ITO-coated glass substrates. The nematic liquid crystal 5CB forms the core region, which is surrounded by a negative photoresist AZ15nXT as the cladding. The experimental results show that light converges and diverges periodically on propagation through the LC core PSW when an external voltage is applied to the periodically segmented electrodes. We fabricated four LC core PSWs, with different duty cycles of 0.25, 0.33, 0.50 and 0.76, and analyzed the propagation characteristics in terms of the output power and effective refractive index.

[1] Author to whom any correspondence should be addressed.

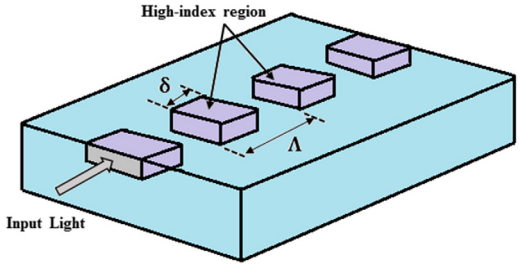

Figure 1. Schematic of a periodic segmented waveguide with high-index segments of length δ and segmentation period Λ.

2. Design and fabrication of LC core PSW

The LC core PSW consists of a guiding layer of the LC 5CB ($n_o = 1.53$, $n_e = 1.71$ at $\lambda = 633$ nm), surrounded by cladding layers of the polymer AZ15nXT ($n_{cl} = 1.60$), and sandwiched between two ITO-coated glass plates. The thickness of ITO layer is ~150 nm, and the refractive index of the glass (Corning Gorilla glass) is 1.51 at 633 nm wavelength. The absolute value of the period of segmentation (Λ) for all the fabricated LC core PSWs is 2 mm. Figure 2(a) shows a schematic of the two ITO-coated glass plates (before bonding), with the various polymer layers and the periodically segmented electrode; on bonding the two glass plates, it forms a hollow rectangular core waveguide, which is then filled by the LC 5CB. Figure 2(b) shows a schematic of the cross section of an LC core PSW with the two constituent ITO-coated glass plates bonded together; the figure also shows a qualitative representation of the refractive index profile along the vertical dashed line.

The periodically segmented electrode pattern, with duty cycles of 0.25, 0.33, 0.50 and 0.76 were imprinted in four different samples of ITO-coated glass substrates by a two-level lithographic process. In the first level lithography, the periodically segmented structures with required duty cycles were fabricated on the lower ITO-coated glass substrate by using appropriate masks for the electrode pattern. For masking the required area (to form the segmented electrodes), a positive photoresist (AZ1518 from MicroChemicals, Gmbh) was spin coated on the substrate, which was followed by UV-exposure and development. After this, the unmasked area on the ITO layer was etched by using a chemical solution (HCL + Zn dust) to obtain the periodic segmented electrode pattern on the substrate; the residual photoresist was removed by acetone. In the second level lithography, the negative photoresist AZ15nXT was spin coated on both the glass plates, to form the cladding layers of thickness 3 μm each, and cured by UV-exposure; similarly, a spacer layer of thickness 5 μm, which determines the thickness of the waveguide core, was formed on the cladding layer of the lower glass plate (see figure 2(a)). A thin 'rubbing layer' of polyimide was spin coated on the treated cladding layer of the upper ITO-coated glass plate; the polyimide layer was then gently rubbed along the surface to facilitate planar alignment of the 5CB LC molecules. The treated ITO-coated glass plates were bonded together using a UV curable adhesive to form the hollow rectangular core waveguide. The hollow core region was then infiltrated by the nematic LC

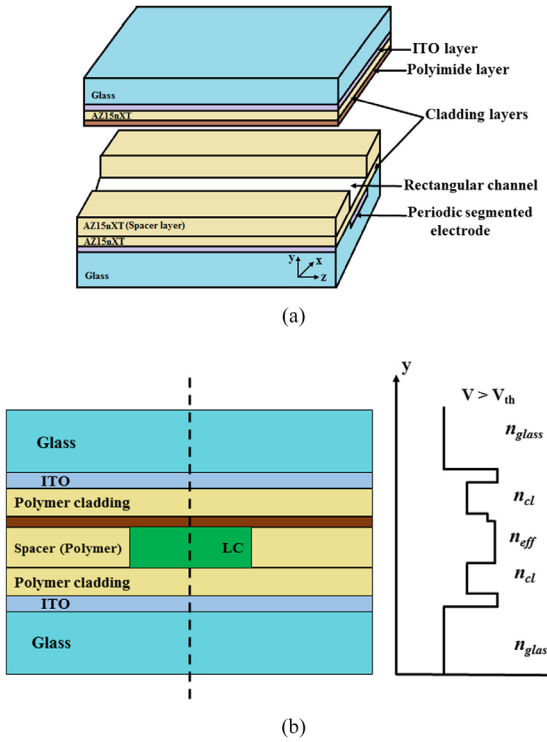

Figure 2. (a) Schematic showing the composition of the two ITO-coated glass substrates with the polymer layers, which form the hollow rectangular core waveguide that is filled with the LC 5CB; (b) schematic of the cross section of an LC core PSW with the two constituent ITO-coated glass plates put together. A qualitative representation of the refractive index profile along the vertical dashed line is also shown alongside.

5CB through the capillary action [21]. Thus, the fabricated LC core waveguide has a rectangular core of 5CB with thickness 5 μm, width 2 mm, and length 10 mm. Since the width of the waveguide is much larger than the thickness, the structure behaves almost like a planar waveguide.

Figure 3(a) shows a schematic representation of the formation of the LC core PSW due to the applied electric field, and figure 3(b) shows a 3D schematic of the electrodes, to realize application of a periodic electric field. When the external electric field is applied to the periodically segmented electrodes, the liquid crystal 5CB molecules re-orient in the direction of the field; no change occurs in the orientation of the LC molecules in the regions bereft of the ITO layer (in the lower glass plate). This results in a periodic index change along the waveguide, forming the LC core PSW.

3. Experiment

A schematic of the experimental set up to characterize the LC core PSWs is shown in figure 4.

In the experiment, light from a He–Ne laser ($\lambda = 632.8$ nm) is passed through a polarizer and a half-wave plate, and then coupled into the LC core PSW through a 20× microscope objective (MO), and coupled out by a 40× MO. The output power is measured by a photodetector, attached to a power meter. Light propagation through the LC core PSW was recorded by a CCD camera, which is attached to a computer.

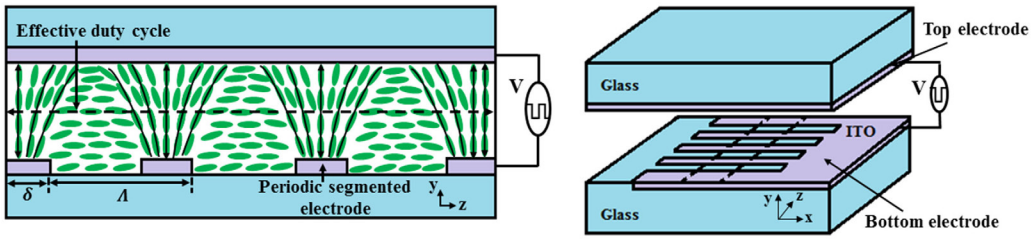

Figure 3. (a) Schematic representation of the longitudinal cross section of the LC core PSW showing formation of periodic domains of different molecular orientation due to the applied electric field; (b) 3D schematic of the electrodes on the ITO coated glass plates.

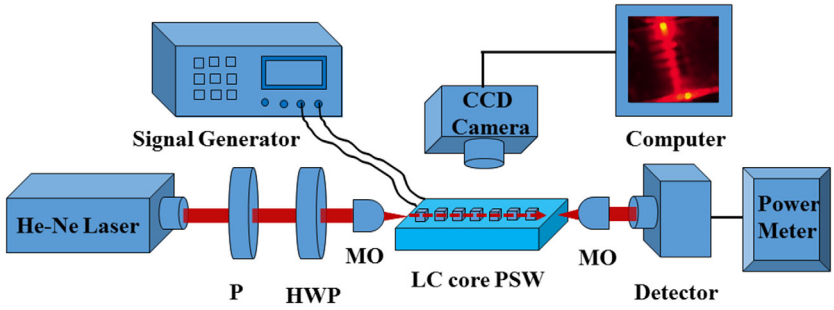

Figure 4. Schematic of the experimental set up to characterize the LC core PSWs; P: polarizer; HWP: Half-wave plate; MO: microscope-objective.

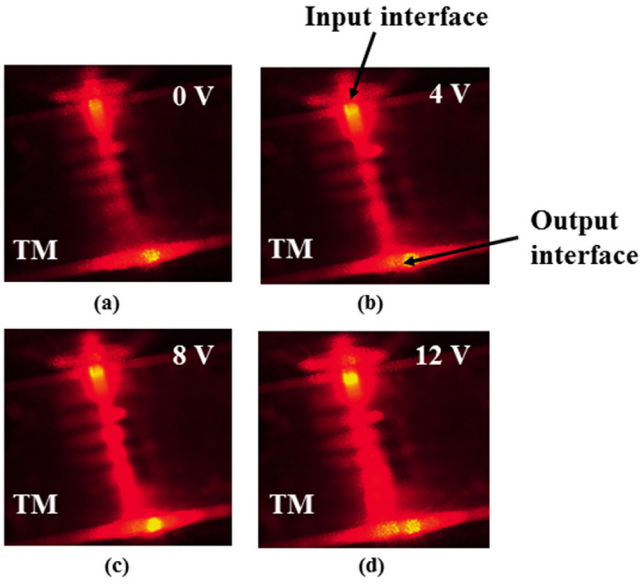

Figure 5. Light propagation through the LC core PSW (top view) with applied voltage V for (a) 0 V, (b) 4 V, (c) 8 V and (d) 12 V.

To study the propagation characteristics of the PSW, a variable square-wave voltage of frequency 1 kHz is applied to the electrodes.

4. Results and discussion

Figures 5(a)–(d) show the top view of light propagation through a LC core PSW with applied voltages of $V = 0$, 4 V, 8 V and 12 V. All snapshots were taken without changing any input/output conditions, except the applied voltage. From the figure, one can see that light diffracts and re-focuses periodically on propagation through the PSW.

Figure 6 shows the variation of the measured output power and the calculated values of the effective extraordinary refractive index of the LC with the applied voltage; the duty cycle for a LC core PSW of duty cycle is 0.50. It can be seen that when $V = 0$, the output power is close to zero, since no guided mode is supported by the LC core PSW. The effective refractive index of the core of the equivalent slab waveguide is approximately given by [9]:

$$n_{\text{eff}} = n_{\text{e}}(\theta)\gamma + (1-\gamma)n_{\text{o}} \tag{1}$$

where γ is the duty cycle of the LC core PSW, n_{o} and $n_{\text{e}}(\theta)$ are the ordinary and the effective extraordinary refractive indices of the LC 5CB; θ is the orientation angle of the LC molecules with respect to the direction of propagation of light; $n_{\text{e}}(\theta)$ is given by [13]:

$$n_{\text{e}}(\theta) = \frac{n_{\text{o}}n_{\text{e}}}{\sqrt{n_{\text{o}}^2\cos^2(\theta) + n_{\text{e}}^2\sin^2(\theta)}} \tag{2}$$

$n_{\text{e}}(\theta)|_{\text{min}} = n_{\text{o}} = 1.53$ (for $\theta = 0$); $n_{\text{e}}(\theta)|_{\text{max}} = n_{\text{e}} = 1.71$ (for $\theta = 90°$). In the fabricated LC core PSWs, the guiding condition for light propagation is satisfied for $n_{\text{cl}} < n_{\text{eff}} \leqslant n_{\text{e}}$. In the absence of an applied voltage (i.e. $V = 0$), all LC molecules are oriented along the z-axis, and therefore both TE (horizontal) and TM (vertical) polarizations see the ordinary refractive index n_{o} (=1.53), which is less than the cladding refractive index n_{cl} (=1.60). As the applied voltage increases to a certain value, called the 'threshold voltage', the effective refractive index n_{eff} increases from n_{o} to $n_{\text{eff}} > n_{\text{cl}}$; at this point, the effective refractive index of the core seen by the TM polarization is greater than that of the cladding, and the guiding condition is satisfied for the LC core PSW. The output power increases rapidly with the applied voltage till $n_{\text{e}}(\theta)$ approaches n_{e}, and then saturates. However, the TE polarization continues

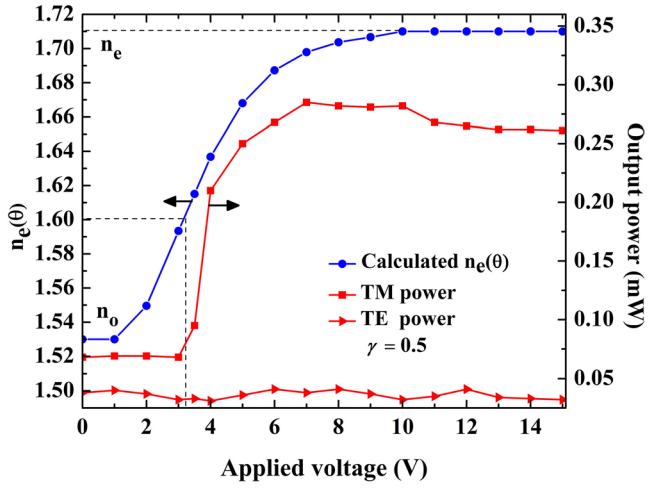

Figure 6. Variation of the calculated effective extraordinary refractive index $n_e(\theta)$ and the measured output power of a LC core PSW with applied voltage for a duty cycle of 0.5.

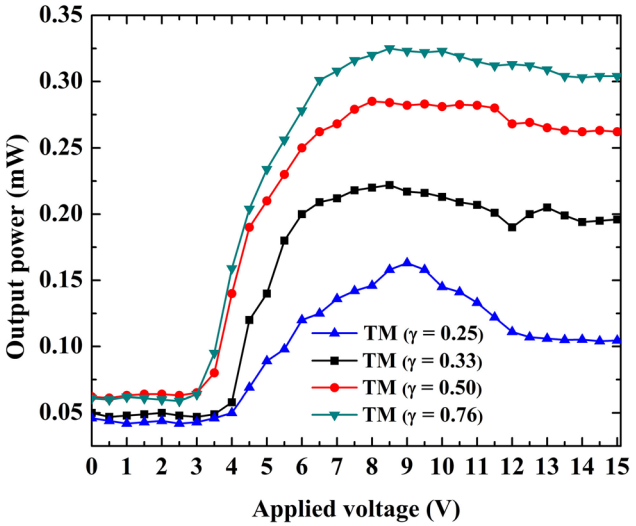

Figure 7. Variation of the output power with applied voltage for four different LC core PSWs with duty cycles (γ) of 0.25, 0.33, 0.50 and 0.76.

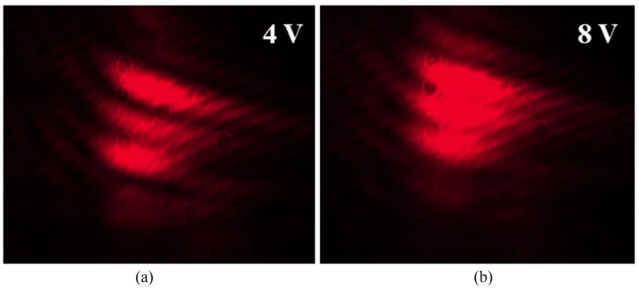

Figure 8. Intensity pattern at the output of the LC core PSW of duty cycle 0.50 with applied voltage V for (a) 4 V and (b) 8 V with the same field of view.

to see the same ordinary refractive index, and therefore there is no guided TE mode in the LC core PSW. Thus, the output power in the TE polarization does not show any significant variation with the applied voltage.

The measured variation of the output power (see figure 6) explains the power variations seen in figures 5(a)–(d). The transverse scattered power (captured by the CCD camera) is proportional to the guided power through the LC core PSW. Since the waveguide is only 10 mm long, some amount of partially reflected and scattered light would reach the output end, contributing to non-zero output at $V = 0$, although there is no waveguide. At 4 V, which is close to the threshold voltage, the output power increases for the TM polarization due to onset of the wave guidance. The output power further increases at the higher voltages of 8 V and 12 V because now the waveguide supports a greater number of higher order modes, and more and more power gets coupled into the LC core PSW.

Figure 7 shows the variation of the measured output power with the applied voltage for four LC core PSWs of different duty cycles. As can be seen from the figure, the measured threshold voltage varies with the duty cycle; as the duty cycle increases, the threshold voltage decreases, as expected (see equation (1)). For larger duty cycles, the effective refractive index of the core is higher for a given voltage. The measured output power increases with increase in the duty cycle, since the V-parameter [27] of the LC core PSW increases with the effective refractive index:

$$V = \frac{2\pi}{\lambda} d \sqrt{n_{\text{eff}}^2 - n_{\text{cl}}^2} \tag{3}$$

where d is the waveguide thickness. Waveguides with higher values of V support a greater number of guided modes, and hence the input power accepted into the guided mode will be higher.

We calculated the total insertion loss (IL) given by [21]:

$$\text{IL} = 10 \log \frac{P_{\text{out}}}{P_{\text{in}}} \tag{4}$$

where P_{in} and P_{out} are the measured powers at the output of the 20× MO (before coupling into the PSW) and at the output end of the PSW, respectively. The measured insertion losses are 12.7 dB, 11.4 dB, 10.3 dB, and 9.7 dB for duty cycles of 0.25, 0.33, 0.50 and 0.76, respectively, at an applied voltage of 9 V; as expected, the insertion loss is lower for waveguides with higher duty cycles since the effective numerical aperture of PSWs with higher duty cycle are larger. The relatively higher insertion loss is primarily due to input/output coupling losses, and we expect to reduce the insertion loss further by devising a better end-face of the LC core PSW.

Figures 8(a)–(b) show the intensity pattern recorded at the output end of the LC core PSW of duty cycle 0.50 with applied voltages of 4 V and 8 V; both snapshots were taken without changing any input/output conditions, except the applied voltage. The intensity pattern appears as horizontal bands rather than a spot because the width of the fabricated waveguide is much larger than the thickness, and the LC core PSW supports multimode propagation. The effective refractive index of the LC core PSWs are controlled by the applied voltage, and hence the guided mode size can be electrically tuned. This inherent feature can be used effectively to design dynamic mode size converters. Towards this end, efforts are underway to fabricate single mode LC core PSW.

5. Conclusion

We have presented the fabrication and characterization of electrically-tunable LC core PSWs, with four duty cycles of 0.25, 0.33, 0.50 and 0.76. The performance of the LC core PSWs are experimentally and numerically analyzed, in terms of the dependence of the effective refractive index and output power on the duty cycle of the segmentation. The experimental result shows that the fabricated device works as a polarizer and mode size converter for the TM polarization, with potential applications in photonics.

Acknowledgment

The authors would like to thank the Government of India, Ministry of Defence, Defence Research and Development Organization, New Delhi, for financial support to this project (ERIP/ER/1400474/M/01/1571).

References

[1] Halir R 2015 Waveguide sub-wavelength structures: a review of principles and applications *Laser Photonics Rev.* **9** 25–49
[2] Bierlein J D, Laubacher D B, Brown J B and Van der Poel C J 1990 Balanced phase matching in segmented $KTiOPO_4$ waveguides *Appl. Phys. Lett.* **56** 1725–7
[3] Vander Poel C J, Bierlein J D and Brown J B 1990 Efficient type I blue second harmonic generation in periodically segmented $KTiOPO_4$ waveguides *Appl. Phys. Lett.* **57** 2074–6
[4] Li L and Burke J J 1992 Linear propagation characteristics of periodically segmented waveguides *Opt. Lett.* **17** 1195–7
[5] Thyagarajan K, Mahalakshmi V and Shenoy M R 1994 Propagation characteristics of planar segmented waveguides with parabolic index segments *Opt. Lett.* **19** 2113–5
[6] Baldi P, Shenoy M R, Nouh S, De Micheli M P and Ostrowsky D B 1994 Estimation of the extent and influence of longitudinal diffusion on $LiNbO_3$ proton exchanged segmented strip waveguides *Opt. Commun.* **104** 308–12
[7] Chou M H, Arbore M A and Fejer M M 1996 Adiabatically tapered periodic segmentation of channel waveguides for mode-size transformation and fundamental mode excitation *Opt. Lett.* **21** 794–6
[8] Weissman Z and Hardy A 1993 Modes of periodically segmented waveguides *J. Lightwave Technol.* **11** 1831–7
[9] Thyagarajan K, Mahalakshmi V and Shenoy M R 1995 Equivalent waveguide model for parabolic index planar segmented waveguides *Opt. Comm.* **121** 27–30
[10] Aschiéri P, Rastogi V, Chanvillard L, Baldi P, Micheli M P D, Ostrowsky D B, Bellanca G, Bassi P, Thyagarajan K and Shenoy M R 1999 Experimental observation of longitudinal modulation of mode fields in periodically segmented waveguides *Appl. Opt.* **38** 5734–7
[11] Rastogi V, Ghatak A K, Ostrowsky D B, Thyagarajan K and Shenoy M R 1998 Ray analysis of parabolic-index segmented planar waveguides *Appl. Opt.* **37** 4851–6
[12] Mercedes C E R, Esquerre V F R, Lima I T and Figueroa H E H 2014 Analysis of straight periodic segmented waveguide using the 2-D finite element method *J. Lightwave Technol.* **32** 2163–9
[13] Khoo I C 2007 *Liquid Crystals* (New York: Wiley)
[14] Chigrinov V G 2007 Liquid crystal devices for photonics applications *Proc. SPIE* **6781** 67811M
[15] Beeckman J, Neyts K and Vanbrabant P J M 2011 Liquid-crystal photonic applications *Opt. Eng.* **50** 081202
[16] Zografopoulos D C, Asquini R, Kriezis E E, D'Alessandro A and Beccherelli R 2012 Guided-wave liquid-crystal photonics *Lab Chip* **12** 3598–610
[17] D'Alessandro A, Bellini B, Donisi D, Beccherelli R and Asquini R 2006 Nematic liquid crystal optical channel waveguides on silicon *IEEE J. Quantum Electron.* **42** 1084–90
[18] Wang T J, Chaung C K, Li W J, Chen T J and Chen B Y 2013 Electrically tunable liquid-crystal-core optical channel waveguide *J. Lightwave Technol.* **31** 3570–4
[19] Bellini B and Beccherelli R 2009 Modelling, design and analysis of liquid crystal waveguides in preferentially etched silicon grooves *J. Phys. D: Appl. Phys.* **42** 045111
[20] Shenoy M R, Sharma M and Sinha A 2015 An electrically-controlled nematic liquid crystal core waveguide with a low switching threshold *J. Lightwave Technol.* **33** 1948–53
[21] Sharma M, Shenoy M R and Sinha A 2016 A low-loss optical switch using liquid crystal core waveguide with polymer cladding *J. Lightwave Technol.* **34** 3065–70
[22] Komitov L, Hegde G and Kolev G 2011 Fast liquid crystal light shutter *J. Phys. D: Appl. Phys.* **44** 442002
[23] Gardiner D J and Coles H J 2006 Organosiloxane liquid crystals for fast-switching bistable scattering devices *J. Phys. D: Appl. Phys.* **39** 4948–55
[24] Monat C, Domachuk P and Eggleton B J 2007 Integrated optofluidics: a new river of light *Nat. Photon.* **1** 106–14
[25] Huang W, Pu D, Shen S, Wei G, Xuan L and Chen L 2015 Effects of monomer functionality on performances of scaffolding morphologic transmission gratings recorded in polymer dispersed liquid crystals *J. Phys. D: Appl. Phys.* **48** 375303
[26] Sharma M, Shenoy M R and Sinha A 2016 Electrically-controlled periodic segmented waveguide with a nematic liquid crystal core *Photonics and Fiber Technology 2016 OSA Technical Digest Series* AM5C.5
[27] Ghatak A K and Thyagarajan K 1989 *Optical Electronics* (Cambridge: Cambridge University Press)